

New CTIC Correction Method for the Spaced-Row Charge Injection of the Suzaku X-Ray Imaging Spectrometer

Hideki Uchiyama¹, M idori Ozawa¹, Hironori Matsumoto¹,
Takeshi Gotsuru¹, Katsuji Koyama¹, Masashi Kimura²,
Hiroyuki Uchida², Hiroshi Nakajima², Kiyoshi Hayashida²,
Hiroshi Tsunemi², Hideyuki Mori³, Aya Bamba³,
Masanobu Ozaki³, Tadayasu Dotani³, Dai Takei⁴,
Hiroshi Murakami⁴, Koji Mori⁵, Yoshitaka Ishisaki⁶,
Takayoshi Kohmura⁷, Gregory Prigozhin⁸, Steve Kissel⁸,
Eric Miller⁸, Beverly Lamarr⁸, and Marshall Bautz⁸

¹Department of Physics, Graduate School of Science, Kyoto University,
Sakyo-ku, Kyoto 606-8502

E-mail (HU) uchiyam@cr.sphys.kyoto-u.ac.jp

²Department of Earth and Space Science, Osaka University,
Machikaneyama, Toyonaka, Osaka 560-0043

³Institute of Space and Astronautical Science, Japan Aerospace Exploration Agency,
3-1-1 Yoshinodai, Sagamihara, Kanagawa 229-8510

⁴Department of Physics, Rikkyo University,
3-34-1 Nishi-Ikebukuro, Toshima-ku, Tokyo 171-8501

⁵Department of Applied Physics, University of Miyazaki,
1-1 Gakuen Kibana-dai Nishi, Miyazaki 889-2192

⁶Department of Physics, Tokyo Metropolitan University,
1-1 Minamiosawa, Hachioji, Tokyo 192-0397

⁷Department of General Education, Kogakuin University,
2665-1 Nakano-cho, Hachioji, Tokyo 192-0015

⁸Kavli Institute for Astrophysics and Space Research, Massachusetts Institute of Technology,
77 Massachusetts Avenue, Cambridge, MA 02139, USA

(Received 2000 December 31; accepted 2001 January 1)

Abstract

The charge transfer inefficiency (CTI) of the X-ray CCDs on board the Suzaku satellite (X-ray Imaging Spectrometers; XIS) has increased since the launch due to radiation damage, and the energy resolution has been degraded. To improve the CTI, we have applied a spaced-row charge injection (SCI) technique to the XIS in orbit; by injecting charges into CCD rows periodically, the CTI is actively decreased. The CTI in the SCImode depends on the distance between a signal charge and a preceding injected row, and the pulse height shows periodic positional variations. Using in-flight data of onboard calibration sources and of the strong iron line from the Perseus cluster of galaxies, we studied the variation in detail. We developed a new method to correct the variation. By applying the new method, the energy resolution (FWHM) at 5.9 keV at March 2008 is 155 eV for the front-illuminated CCDs and 175 eV for the back-illuminated CCD.

Key words: instrumentation: detectors | techniques: spectroscopic | X-ray CCDs

1. Introduction

X-ray charge coupled devices (CCDs) have good spatial and energy resolution, and they have been the main detector for imaging spectroscopy in X-ray astronomy since the ASCA SIS (Burke et al. 1993). X-ray CCDs in orbit, however, suffer from radiation damage. The damage causes the increase of the charge transfer inefficiency (CTI), which results in the degradation of the energy resolution for two reasons: 1) the pulse height strongly depends on the position of an X-ray event, since the X-ray event loses more electric charges as the number of trans-

fer increases, and 2) the loss of charge is a stochastic process, and thus there is a fluctuation in the amount of lost charge. In the case of the X-ray Imaging Spectrometer (XIS; Koyama et al. 2007) on board the Suzaku satellite (Mitsuda et al. 2007), the energy resolution at 5.9 keV was 140 eV (FWHM) at August 2005, and had degraded to 200 eV at August 2006.

The XIS is equipped with a charge injection (CI) structure (Prigozhin et al. 2004; Bautz et al. 2004; Lamarr et al. 2004; Prigozhin et al. 2008) which lies adjacent to the top row of the imaging area. The CI structure allows us to inject a commandable amount of charge in a nearly

arbitrary spatial pattern. We can measure the CTI of each column precisely by the checkerboard CI technique, and it is possible to correct the lost charge. The column-to-column CTI correction improves the energy resolution greatly (Nakajima et al. 2008; Ozawa et al. 2009). However, we cannot correct the fluctuation in principle, and the degraded energy resolution cannot be fully restored even with the column-to-column correction.

The CI can be used in another way to mitigate the effect of the radiation damage; the spaced-row charge injection (SCI) technique can reduce the CTI actively and improve the energy resolution. In the SCI technique, a charge is injected into CCD rows periodically. The injected charge fills the radiation-induced traps as a "sacrificial charge", and thus prevents some of the traps from capturing a signal charge produced by X-rays. Results based on ground experiments using the SCI technique with radiation-damaged CCDs have been reported (Tomida et al. 1997; Bautz et al. 2004), but no in-orbit experiment had been done. The Suzaku XIS operated with the SCI technique in orbit for the first time at August 2006, and the energy resolution was improved from 200 eV to 140 eV at 5.9 keV (Bautz et al. 2007). The SCI has been a normal observation mode since October 2006.

In this paper, we report the study of the CTI in the SCImode, and present a new CTI correction method. Because the CTI depends on the distance between a pixel and a charge injected row, the calibration for the SCImode becomes complicated. We developed a new method to correct the complex CTI of the SCImode to improve the energy resolution further. We also found that the CTI increased with time even with the SCI, and our method can correct the time variation. All errors are at the 1 confidence level unless otherwise described.

2. Spaced-row Charge Injection

In the SCImode of the Suzaku XIS, a charge is injected into every 54th row. The amounts of the injected charge into each pixel are equivalent to the X-ray energy of 6 keV and of 2 keV, for the front-illuminated (FI) and back-illuminated CCD (BI), respectively.

The terminology and notations for the CCD, CTI, and CI are the same as Ozawa et al. (2009). To make clear for further descriptions of the SCI, relevant terminology and notations are summarized in table 1.

The CTI in the SCImode is assumed to consist of two components as CTI1 and CTI2 following Ozawa et al. (2009). The relation among readout pulse height (PH^0), original pulse height generated by an X-ray of energy E (PH_0 at E), CTI1 (c_1), CTI2 (c_2), and transfer number i are formalized in equation 2 of Ozawa et al. (2009), where the detector coordinates are defined as ActX and ActY. The CCD consists of four segments (A, B, C, and D); each segment consists of 256 columns along ActX and has a dedicated read-out node.

In the SCImode, a radiation-induced trap is filled with a probability p when a sacrificial charge passes through the trap. The filled trap does not capture a signal charge

produced by an X-ray. However, the electron once filling the trap will be re-emitted with the time scale τ . Thus the probability of the trap holding the electron is proportional to $p \exp(-t/\tau)$, where t is the time elapsed since the sacrificial charge passes the trap. Thus it is reasonable to assume that a pixel which is j rows away from its preceding charge injected row has the c_1 value proportional to $1 - p \exp(-t_j/\tau)$, where t_j is time for one vertical transfer; t_j represents a time lag between the pixel and the charge injected row. We assume t_j/τ is a small value, and hence $1 - p \exp(-t_j/\tau)$ is a linear function of j approximately. The charge is injected into every 54th row, and hence $j = i \bmod 54$ ¹. We, consequently, can model the c_1 - i relation of the SCImode as,

$$c_1(i) = c_{1t} + \frac{c_{1b} - c_{1t}}{54} (i \bmod 54): \quad (1)$$

Equation 1 is a periodic sawtooth function as demonstrated in figure 1a. This c_1 - i relation generates the PH^0 - i relation in figure 1b, and the shape is nicely reproduced by the ground experiments using the heavily damaged CCD as demonstrated in figure 15 of Tomida et al. (1997).

The sawtooth distribution is also found in the XIS in-orbit. We measured the PH^0 - i relations using the onboard calibration source data in October 2006 with an effective exposure time of 1 Ms, and show the results in figures 2a and b. Figure 2 shows that the sawtooth of the BI sensor is shallower than that of the FI sensors. The results based on the data in February 2008 are also shown in figures 2c and d. Compared with October 2006, the sawtooth became deeper. The pulse height just after the charge injected rows changed more in the case of the BI sensor than the FI sensors. This difference might be resulted in part from the smaller amount of charge injected in the BI sensor.

Our sawtooth CTI model can represent the complicated relation between PH^0 and i , and make it possible to convert $PH^0(i)$ to PH_0 with only three parameters, c_{1t} , c_{1b} , and c_2 . Our goal is to convert $PH^0(i)$ to PH_0 by deciding the three parameters.

3. CTI Measurement in Orbit

3.1. Calibration Data

To study the CTI in the SCImode, we analyzed the data of the onboard calibration sources ⁵⁵Fe, the Perseus cluster of galaxies, and 1E 0102.2-7219, whose properties are summarized in section 4 of Ozawa et al. (2009).

XIS 2 suddenly showed an anomaly on November 9, 2006, and it has not been operated since then. Although there is no direct evidence, the micro-meteoroid impact might have caused the anomaly². Thus only the data of XIS 0, 1 and 3 are studied.

¹ The modular arithmetic $i \bmod 54 = j$ means that when i is divided by 54, it leaves j as the remainder, hence $i - j$ is divisible by 54. For example, $111 \bmod 54 = 3$. Strictly speaking, charges are injected in rows of $i = 54n + 1$ ($n = 0; \dots; 18$) and 1023 for full window mode. Thus j should be $(i + 1) \bmod 54$. We nevertheless use this simplified description to avoid unnecessary confusion. We treated j properly for actual CTI measurement.

² See <http://www.astro.isas.jaxa.jp/suzaku/proposal/ao3/suzaku-td/>.

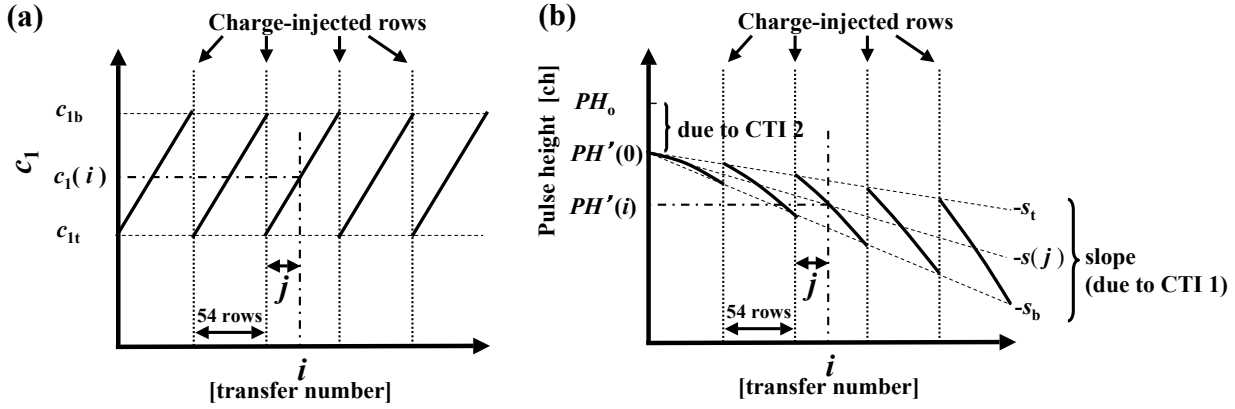


Fig. 1. Schematic model of the "saw tooth" variation. We assume the c_i - i relation shown in (a), and it generates the PH' - i relation shown in (b).

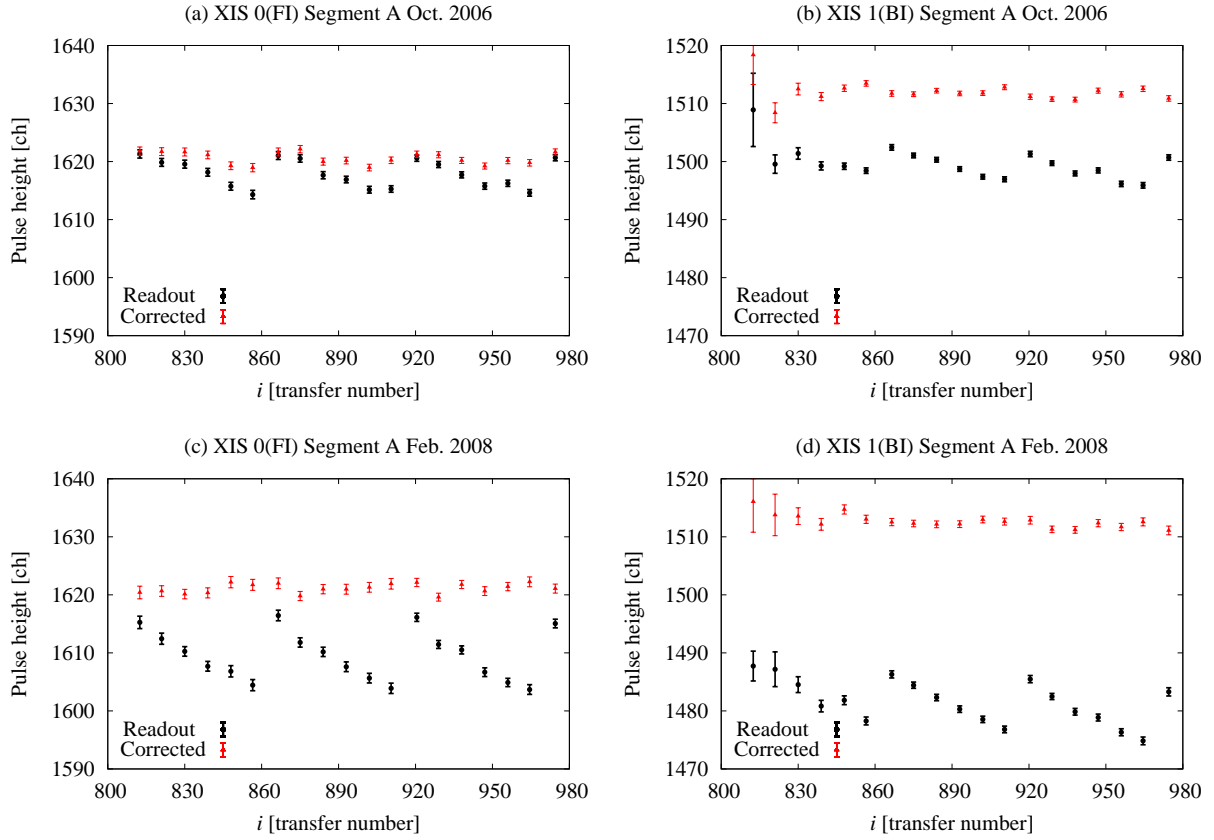


Fig. 2. Pulse height of the Mn K line from the onboard calibration source as a function of i : October 2006 (a and b) and February 2008 (c and d). We show the results of the segment A in XIS 0, 1 as typical examples. X-ray events of grade 02346 were analyzed. Black and red marks are data before and after our new CTI correction, respectively.

Table 1. The list of notation.

Notation	Meaning
i	Transfer number. $i = \text{ActY} + 1$; ActY is a coordinate value where an incident X-ray generates a charge.
PH_0	Original pulse height.
$\text{PH}^0(0)$	Readout pulse height of a pixel at $i = 0$. It is equal to $(1 - 1024 \cdot \varphi) \text{PH}_0$.
$\text{PH}^0(i)$	Readout pulse height of a pixel at i .
j	Row number between a pixel and its preceding charge injected row. $j = i \bmod 54$:
$c_1(i)$	CTI1 of Ozawa et al. (2009) for a pixel at i .
c_{1t}, c_{1b}	The c_1 values at the peak and valley of the sawtooth (see figure 1a).
c_2	CTI2 of Ozawa et al. (2009).
$s(j)$	Slope for a pixel with j . It is equal to $c_1(i) \text{PH}_0$.
s_t	Slope for the tops of the sawtooth. It is equal to $c_{1t} \text{PH}_0$.
s_b	Slope for the bottoms of the sawtooth. It is equal to $c_{1b} \text{PH}_0$.
	CTI depends on the pulse height as $c_{1;2} / \text{PH}_0$. See Ozawa et al. (2009).

All data were acquired with the normal clocking mode and the full window option using the SCI. The editing mode was 3-3 or 5-5. Koyama et al. (2007) provide details of these modes.

As mentioned in Koyama et al. (2007), a small fraction of the charge in a pixel is left behind (trailed) to the next pixel during the transfer. This charge-trail phenomenon changes the spatial extent of an X-ray event. All data were corrected for the phenomenon based on the in-orbit data³, otherwise some X-ray events would be judged as grade 7, and the detection efficiency would decrease.

We used the archival trend data of the calibration source obtained between August 2006 and March 2008, and the total effective exposure time is about 23.7 Ms. The observations of the celestial objects are summarized in table 2.

3.2. Determination of the CTI Parameters

The procedures for the CTI determination are as follows:

- Step 1: deciding PH_0 at 5.895 keV and 6.56 keV.
- Step 2: measuring φ for PH_0 at 6.56 keV.
- Step 3: measuring φ_t and c_{1b} for PH_0 at 5.895 keV or 6.56 keV.
- Step 4: deciding the CTIs for any PH^0 values.

In the case of the non-SCI mode, we can measure the CTI of each column by the checkerboard CI (Nakajima et al. 2008; Ozawa et al. 2009). Since the checkerboard CI is a complicated operation, we have not used this technique in the SCI mode. We, therefore, measured the averaged CTI of each segment.

In the normal analysis of the XIS data, both of single-pixel and multi-pixel events (grade 0 and 2346 events; see Koyama et al. 2007) are used. To determine the CTI, however, we analyzed only the grade 0 events; if we use the multi-pixel events, it is difficult to measure the CTI correctly, because the CTI depends on the amount of transferred charge, and the amounts of charge in each pixel comprising the multi-pixel event is different with

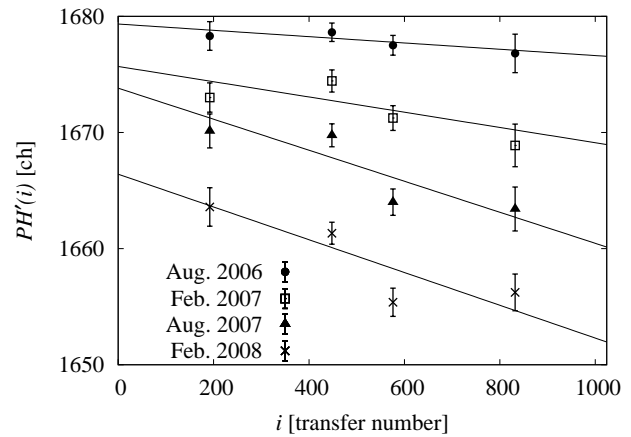


Fig. 3. PH^0 as a function of i obtained using the Fe xxv K α line from the Perseus cluster. The result of the XIS 1 segment C is shown as a typical example.

each other. We will mention how to correct the data of grade 02346 events in step 4.

- Step 1: PH_0 at 5.895 keV and 6.56 keV

We determined the PH_0 s of the Fe xxv K α line from the Perseus cluster (6.56 keV) by using the data of the first SCI observation on 29 August, 2006. Because it is impossible to measure the c_2 value in August 2006, we assumed that value is equal to zero. Even if this assumption would not be reasonable, we can cover it by adjusting the PH_0 -E relation. Then the PH^0 at $i = 0$ ($\text{PH}^0(0)$) is equal to PH_0 .

Since the statistics are limited, we divided each segment to four regions along the ActY axis, and obtained the center pulse height of the iron line from each region. An example of PH^0 as a function of i is shown in figure 3. By fitting the data with a linear function of i , the PH_0 value was obtained as $\text{PH}^0(0)$.

For the segments A and D, we obtained the PH_0 value of the Mn K α line (5.895 keV) using the data of the calibration sources in August, 2006. We obtained the PH^0 - i relation, but in this case, the i values are limited at around 900 because the calibration sources irradiate

³ The details about the charge-trail correction is shown in http://xmm2.esac.esa.int/external/xmm_sw_cal/icw/g/presentations/Suzaku-XIS.pdf

Table 2. Log of Observations for Calibration.

Obs. ID	Observation time (UT)		Exposure time [ks]
	Start	End	
The Perseus cluster			
101012010	2006/08/29 18:55:07	2006/09/02 01:54:19	50.0
101012020	2007/02/05 15:57:48	2007/02/06 14:30:14	43.9
102011010	2007/08/15 12:40:49	2007/08/16 11:27:22	42.3
102012010	2008/02/07 02:09:42	2008/02/08 10:30:19	41.6
1E 0102.2-7219			
101005090	2006/12/13 18:53:16	2006/12/14 03:04:19	28.2
101005110	2007/02/10 22:13:47	2007/02/11 19:30:14	36.2
102001010	2007/04/10 10:35:08	2007/04/10 19:30:19	18.1
102002010	2007/06/13 10:10:12	2007/06/14 03:31:19	27.9
102003010	2007/08/12 05:21:09	2007/08/13 03:45:24	39.5
102004010	2007/10/25 12:24:45	2007/10/26 09:00:14	26.2
102005010	2007/12/01 19:25:40	2007/12/02 09:50:19	24.8
102022010	2008/02/14 16:57:28	2008/02/16 03:10:24	26.5
102006010	2008/03/15 05:43:27	2008/03/15 20:45:24	28.2

only the two far-end corners from the read-out node of the imaging area (Koyama et al. 2007). We extrapolated the relation to $i = 0$ by using a linear function, the slope of which was fixed to a value s_{Mn} calculated as follows. Because the slope represents an averaged c_1 for PH_0 , the slope should be proportional to PH_0^{-1} . Then we calculated s_{Mn} from the slope for the 6.56 keV data (s_{Fe}) as $s_{\text{Mn}} = s_{\text{Fe}} (5.895/6.56)^{-1} = s_{\text{Fe}} (0.90)^{-1}$.

Step 2: c_2 for PH_0 at 6.56 keV

We obtained the $\text{PH}^0(0)$ values for all data of the Perseus cluster (table 2) with the same method of step 1. The PH^0 - i relations are shown in figure 3. As is found in figure 3, $\text{PH}^0(0)$ is decreased with time; $\text{PH}^0(0)$ becomes different from PH_0 . We assumed the difference $\text{PH}_0 - \text{PH}^0(0)$ is attributable to c_2 . Assuming that c_2 is a linear function of time, the increasing rate of c_2 for PH_0 (at 6.56 keV) is typically $2 \times 10^{-6} \text{ yr}^{-1}$ for the FI sensors and $6 \times 10^{-6} \text{ yr}^{-1}$ for the BI sensor.

Step 3: c_{1t} and c_{1b} for PH_0 at 5.895 keV and 6.56 keV

For the segments A and D, we determined s_t and s_b for PH_0 at 5.895 keV by using the data of the calibration sources. For the segments B and C, we measured those for PH_0 at 6.56 keV by using the Perseus data. We fitted the PH^0 - i relation with the sawtooth function shown in figure 1b, and determined s_t and s_b . In the fitting, we fixed the PH_0 and c_2 to the values obtained in step 1 and step 2. Typical examples of the fitting are shown in figures 4 and 5. Using s_t and s_b , we calculated c_{1t} and c_{1b} .

In the case of the FI sensors, the c_{1t} and c_{1b} values for PH_0 at 5.895 keV at August 2006 are typically $< 10^{-7}$ and 3×10^{-6} , respectively. The increasing rates are $1 \times 10^{-6} \text{ yr}^{-1}$ and $5 \times 10^{-6} \text{ yr}^{-1}$, respectively. In the case of the BI sensor, the parameters c_{1t} and c_{1b} at August 2006 are 6×10^{-6} and 1×10^{-5} , and the increasing rates are $5 \times 10^{-6} \text{ yr}^{-1}$ and $8 \times 10^{-6} \text{ yr}^{-1}$,

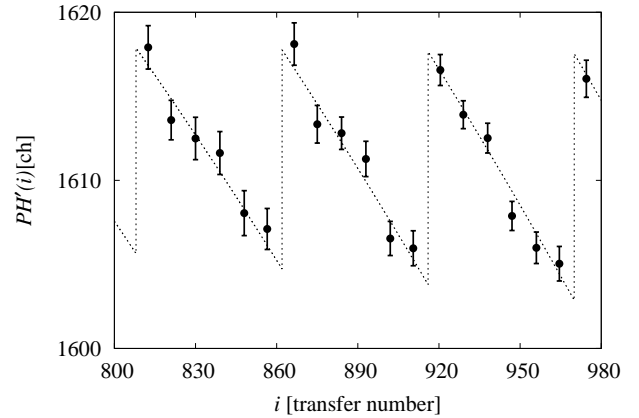


Fig. 4. Best-fitting result of the sawtooth function for the Mn K line of the calibration source. The result of the XIS 0 segment A in February 2008 is shown as a typical example. Only grade 0 events were used.

respectively. Typical examples of the time evolution of the c_1 values for PH_0 at 5.895 keV are shown in figure 6.

The CTI of the BI sensor is larger, and increases more rapidly than that of the FI sensors. It might be the reason that the amount of the injected charge to the BI sensor is less than that of FIs.

Step 4: CTI for any PH^0 values

For an event of PH^0 , we calculated the CTI with an equation of $c_{1;2}$, $\text{fPH}^0 = (\text{PH}_0 \text{ at } 5.895 \text{ keV or } 6.56 \text{ keV}) g$. Here, we assumed the same PH_0 - $c_{1;2}$ relation as that of the non-SCI mode and used the same (typically 0.25; Ozawa et al. 2009).

Since we obtained the CTI for all pulse-height values, we can now correct the CTI of multi-pixel events (grade 2346 events). By using the Mn K line of the calibration sources or the Fe xxv K line from the Perseus cluster, we examined the CTI correction for the grade 02346

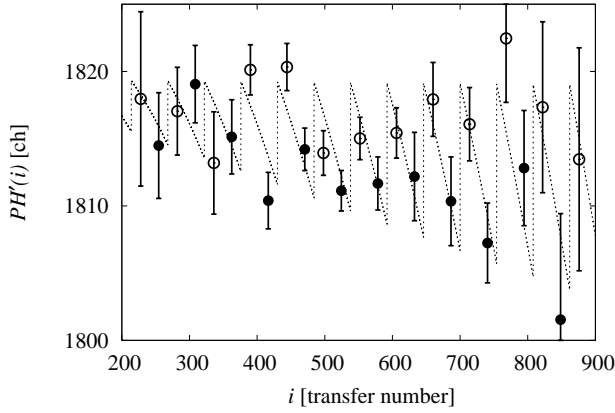


Fig. 5. Best-fitting result of the sawtooth function for the Fe xxv K line from the Perseus cluster. The result of the XIS 0 segment C in February 2008 is shown as a typical example. The white and black circles show the pulse height of regions with smaller and larger j values, respectively. Only grade 0 events were used.

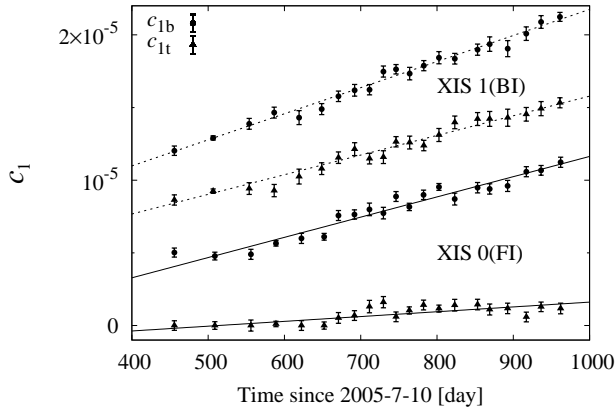


Fig. 6. Time history of c_{1t} and c_{1b} for PH_0 at 5.895 keV. The segment A of XIS 0 and 1 are shown as typical examples.

events. Figure 7 shows the line centroid of the grade 0 and grade 02346 events as a function of time. While the line centroid of the grade 0 events is temporally constant, that of the grade 02346 events increases with time. This means that the CTI parameters for the grade 2346 events are smaller than those for the grade 0 events. The CTI of the grade 2346 events can be smaller, because the split charge acts as the sacrificial charge.

We then re-tuned the parameters q_t , c_{1b} , and c_2 by multiplying a common time-independent factor. We determined the factor of each segment so that the line center of the grade 02346 events becomes temporally constant. The factors are typically 0.9. Figure 7 also shows that the result of the grade 02346 data corrected with the re-tuned CTI parameters. The adjusted pulse height becomes constant. However, as a result, the value becomes different from PH_0 measured in step 1. We regarded this adjusted pulse height as PH_0 at 5.895 keV, and determined the PH_0 -E relation.

To check the CTI correction in the low-energy band, we

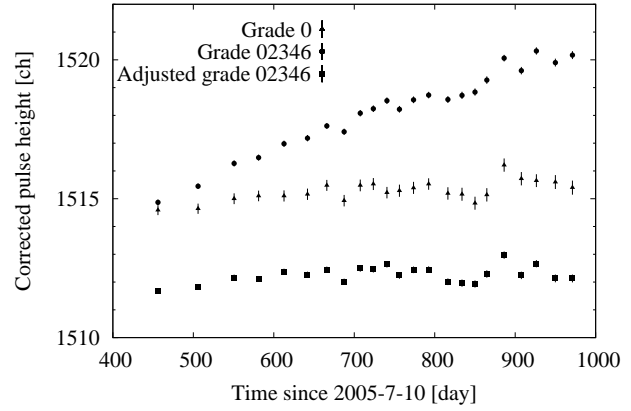


Fig. 7. Time history of the line centroid of Mn K line. We show the result of the XIS 1 segment A as a typical example. The triangle and circle marks show the data of grade 0 and 02346 after the CTI correction with the parameters based on only the grade 0 events. The rectangle marks show the data of grade 02346 events after the CTI correction with the re-tuned parameters as described in the text.

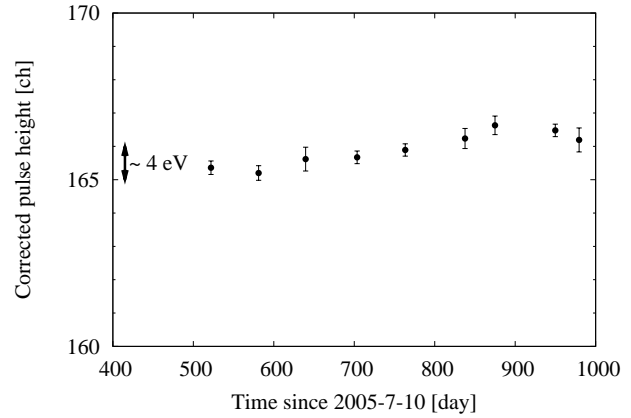


Fig. 8. Time history of the line centroid of O v K (0.653 keV). We show the result of the XIS 1 segment C as a typical example. The results are based on the grade 02346 events corrected with the re-tuned CTI parameters as described in the text.

applied the re-tuned CTI parameters to the grade 02346 data of 1E 0102.2-7219. We fitted the spectrum with the empirical calibration model⁴. Figure 8 shows the pulse height of the O v K line after the CTI correction. We can see that the line centroid is constant, which supports the validity of our method.

4. Energy Scale Uniformity and Resolution in the SCIMode

The pulse height of the Mn K line after our new CTI correction is shown in Figure 2. The sawtooth structure disappeared, and hence our new method greatly reduces the variation of the pulse height. Comparing between October 2006 and February 2008 shows that the CTI vari-

⁴ See <http://cxc.harvard.edu/acis/E0102/>

ation with time is also corrected properly.

The P_{H_0} -E relation for each segment is assumed to be the same function form with a similar re-tuning process of the absolute energy as Ozawa et al. (2009): a model of two slopes crossing at the energy of the Si-K edge (1.839 keV) with the same ratio of the two slopes as that obtained in the ground experiments (Koyama et al. 2007).

The time histories of the energy resolution of the corrected data are shown in figure 9. At the high energy (5.895 keV), the energy resolution of XIS 0 at March 2008 is improved from 160 eV to 155 eV by the sawtooth correction. On the other hand, the energy resolution of XIS 1 at March 2008 is not improved in spite of the sawtooth correction, and stays at 175 eV. At the low energy (0.653 keV), no clear effect of the sawtooth correction is seen in both FI and BI. The energy resolutions at March 2008 are 53 eV (XIS 0) and 62 eV (XIS 1) independently of the correction.

As we mentioned in section 2, the sawtooth of the BI sensor is shallower than that of the FI sensors. We think it causes the difference of the effect of the sawtooth correction between BI and FI. We speculate, at the low energy, the effect of the sawtooth correction was not seen because the original degradation of the energy resolution was small. In fact, the energy resolutions at OVIII K are almost same between the SCIM and non-SCIM mode.

The results of our new method to correct the sawtooth structure has been implemented to the software package released by HEASARC⁵ since HEASoft version 6.3. Now, all of the XIS data of the SCIM mode after the processing version 2.0 are corrected by the sawtooth method.

We thank all the Suzaku team members for their support of the observation and useful information on the XIS calibration. Thanks Dr. Junko Hiraga of RIKEN for her beneficial comments. H.J., M.O., H.J., H.N., A.B., and D.T. are supported by JSPS Research Fellowships for Young Scientists. H.M. is supported by the MEXT, Grant-in-Aid for Young Scientists (B), 18740105, 2008, and is also supported by the Sumitomo Foundation, Grant for Basic Science Research Projects, 071251, 2007. H.T. and K.H. were supported by the MEXT, Grant-in-Aid 16002004. This work was supported by the Grant-in-Aid for the Global COE Program "The Next Generation of Physics, Spun from Universality and Emergence" from the Ministry of Education, Culture, Sports, Science and Technology (MEXT) of Japan.

References

- Bautz, M. W., Kissel, S. E., Prigozhin, G. Y., LaMar, B., Burke, B. E., & Gregory, J. A. 2004, *Proc. SPIE*, 5501, 111
 Bautz, M. W., et al. 2007, *Proc. SPIE*, 6686, 66860Q
 Burke, B. E., Mountain, R. W., Daniels, P. J., Cooper, M. J., & Dolat, V. S. 1993, *Proc. SPIE*, 2006, 272
 Koyama, K., et al. 2007, *PA SJ*, S59, 23

⁵ <http://heasarc.gsfc.nasa.gov/>

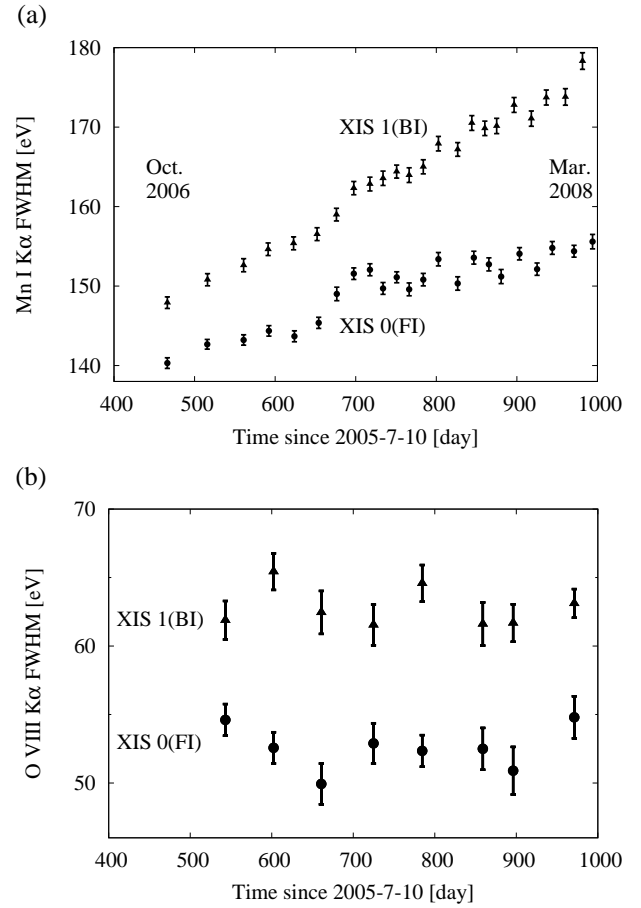


Fig. 9. Time history of the energy resolution (FWHM) at Mn K α (5.895 keV) (a) and at O VIII K α (0.653 keV) (b). The averaged value of the segments A and D are shown for each sensor. The results are based on the grade 02346 events corrected with the re-tuned CTI parameters as described in the text.

- LaMar, B., Bautz, M. W., Kissel, S. E., Prigozhin, G. Y., Hayashida, K., Tsuru, T. G., & Matsumoto, H. 2004, *Proc. SPIE*, 5501, 385
 Mitsuda, K., et al. 2007, *PA SJ*, S59, 1
 Nakajima, H., et al. 2008, *PA SJ*, S60, 1
 Ozawa, M., et al. in prep for *PA SJ*2009
 Prigozhin, G. Y., Burke, B. E., Bautz, M. W., Kissel, S. E., LaMar, B., & Freytsis, M. 2004, *Proc. SPIE*, 5501, 357
 Prigozhin, G., Burke, B., Bautz, M., Kissel, S., & LaMar, B. 2008, *IEEE Transactions on Electron Devices*, vol. 55
 Rasmussen, A. P., Behar, E., Kahn, S. M., den Herder, J. W., & van der Heyden, K. 2001, *A & A*, 365, L231
 Tomida, H., et al. 1997, *PA SJ*, 49, 405